IVYSPRING INTERNATIONAL PUBLISHER

Theranostics

2017; 7(17): 4301-4312. doi: 10.7150/thno.21450

Research Paper

Long-term Effect of Biomineralized Insulin Nanoparticles on Type 2 Diabetes Treatment

Yun Xiao[1, 3], Xiaoyu Wang[2], Ben Wang[3], Xueyao Liu[1], Xurong Xu[2] and Ruikang Tang[1, 2]✉

1. Center for Biomaterials and Biopathways, Department of Chemistry, Zhejiang University, Hangzhou, Zhejiang 310027, China;
2. Qiushi Academy for Advanced Studies, Zhejiang University, Zhejiang University, Hangzhou, Zhejiang 310027, China;
3. Institute of Translational Medicine, Zhejiang University, Zhejiang University, Hangzhou, Zhejiang 310027, China.

✉ Corresponding author: Professor Ruikang Tang, Department of Chemistry, Zhejiang University, Hangzhou, Zhejiang 310027, China; Tel/Fax: +86-571-87953736; E-mail: rtang@zju.edu.cn

Received: 2017.06.13; Accepted: 2017.08.02; Published: 2017.09.26

Abstract

Intracellular insulin may exhibit a long-term effect in regulating protein synthesis, DNA synthesis, and gene transcription. However, the intracellular delivery of insulin is a great challenge. Here, we describe how a simple biomineralization modification of insulin can transport it into intact cells on a large scale, leading to a long-term therapeutic effect on diabetes mellitus. Using insulin-resistant HepG2 cell and diabetic KKAy mice as models, *in vitro* and *in vivo* assessments have demonstrated that biomineralized insulin nanoparticles can trigger glucose metabolism, and this improvement extends after the treatment. The potential exists to improve the current treatment of type 2 diabetes mellitus through biomineralized modifications of insulin. This study provides a new paradigm of biomimetic nanotechnology for biomedical applications.

Key words: type 2 diabetes; biomineralization; insulin; intracellular delivery.

Introduction

Type 2 diabetes mellitus, a metabolic disorder that is characterized by hyperglycemia in the context of insulin resistance, is considered a chronic and incurable condition [1-3]. Currently, insulin administration is one of the most commonly used clinical treatments for the disease [4-6]. As a principal peptide hormone, insulin plays important roles in the regulation of many metabolic functions in mammals [7, 8]. Most of the biological effects of insulin are generated as a direct result of insulin binding to specific receptors on the plasma membranes of cells and causing the phosphorylation of downstream intracellular substrates [9]. However, insulin can also be internalized into cells, where intracellular insulin activity may lead to long-term effects in regulating protein synthesis, DNA synthesis, and gene transcription [10-12]. It is reasonable to speculate that insulin can treat type 2 diabetes through its intracellular activity. Unfortunately, the intracellular delivery of insulin is a challenging approach that cannot be used in basic research or clinical practice. This lack of applicability is largely because of the inefficiency of insulin in penetrating cells and the quick degradation of insulin when it is trapped in the cytoplasm instead of being released inside cells [13-15].

How can insulin be transported into cells without being degraded? An ideal delivery vector should satisfy the requirements, such as efficient internalization and high stability [16]. Recent nano science developments are poised to utilize existing cellular machinery to facilitate the delivery of a protein into cells [17, 18]. Various materials, such as liposomes [19], polymeric nanoparticles [20], nanotubes [21] and nanocages [22], have been explored as intracellular protein delivery carriers. However, the extensive controversy that surrounds the biosecurity of these artificial materials has cast doubt on their clinical uses. In nature, living organisms can spontaneously produce various

nanocomposites composed of calcium phosphate and calcium carbonate to generate hard tissue through biomineralization [23, 24]. These naturally biomineralized nanomaterials exhibit optimal biocompatibility and bio-friendliness [25].

We suggest an alternative platform based on biomineralization for the intracellular delivery of insulin. The resulting biomineralized nanoparticles consist of insulin and calcium phosphate (CaPi), the major inorganic component of biological bones [26, 27]. The biomineral phase can mediate the internalization of insulin and protect insulin against biological degradation. Due to biomineralization treatment, insulin can enter cells on a large scale, simulating an intracellular mechanism for improving glucose metabolism. Both *in vitro* and *in vivo* experiments have demonstrated that biomineralized insulin can exert a long-term therapeutic effect on insulin resistance, which differs completely from the effect of traditional insulin in its free molecular form. This difference introduces a novel pathway for the treatment of type 2 diabetes through biomineralization-based intracellular insulin therapy.

Materials and Methods

Insulin and *in situ* biomineralization

Human insulin powders (Zhejiang Wanbang Pharmaceutical Co., Ltd., China) were dissolved in Tris-HCl (pH=7.4, Shanghai Double-Helix Biotech Co., Ltd., China) at a concentration of 5 mg/mL. The above-prepared insulin-Tris-HCl (8 μL) was mixed with 1 mL of Dulbecco Modified Eagle Medium (DMEM, Invitrogen, USA) with a final concentration of 40 μg/mL for *in vitro* and *in vivo* use in the following experiments. The *in situ* biomineralization modification was initiated by adding 5 μL of $CaCl_2$ (1.0 M) into 1 mL of insulin-DMEM solution. The abundant calcium ions could trigger a spontaneous mineralization in DMEM, and the reaction solution was incubated at 37 °C with 5% CO_2 for 4 h. The resulting biomineralized insulin nanoparticle (BINP) was further separated through centrifugation (8,000 g, 10 min). As the control experiment, 5 μL $CaCl_2$ (1.0 M) was added into 1 mL of DMEM solution to get calcium phosphate nanoparticles without insulin.

Preparation of BINP with inactive insulin

Insulin solution above was heated in boiling water for 5 min to get inactive insulin. 5 μL $CaCl_2$ (1.0 M) was added into 1 mL of DMEM solution (containing 8 μL 5 mg/mL inactive insulin) to get calcium phosphate nanoparticles with inactive insulin.

Au-Labelled insulin

Au-labelled insulin was synthesized, as previously described [28]. Typically, aqueous HAuCl4 solution (5 mL, 10 mM, 37 °C) was added to an insulin solution (5 mL, 50 mg/mL, 37 °C). NaOH solution (0.5 mL, 1 M) was then added, and the reaction was performed at 37 °C for 24 h.

Characterizations of BINP

Electronic microscopy

BINPs were re-dispersed in ethanol. A drop of the suspension was placed on a carbon-coated copper grid or a silicon plate. The sample was air-dried. TEM and SEM examinations were performed using JEM-1200EX (JEOL, Japan) and JSM-35CF (JEOL, Japan), respectively.

Dynamic Light Scattering (DLS)

A Mastersizer 2000 particle size analyzer (Malvern, UK) was used. A He-Ne laser was operated at 633 nm as a light source, and measurements were performed based on the principles of light scattering. The time-dependent autocorrelation function was derived using a 128-channel digital photon correlator. Particle sizes were calculated with the autocorrelation function using an equation relating diffraction intensity and particle size.

FT-IR

An FTIR-8400S infrared spectrophotometer (Shimadzu, Japan) was used. An approximately 1 mg BINP sample was mixed with 30 mg KBr (medium) to prepare transparent pellets. Spectra were taken in the range of 4,000-400 cm^{-1} with a resolution of 4 cm^{-1}. The spectra of pure insulin, pure CaPi, and a simple mixture of CaPi and insulin were also recorded for comparison.

Thermo gravimetric analysis/differential scanning calorimeter thermo examination (TGA/DSC)

BINP solids were dried at 80 °C for 48 h prior to examination. The samples (5-15 mg) were encapsulated in aluminum pans and analyzed using an SDT-Q600 (TA Instruments, USA) at a heating rate of 10 °C/min from 20 °C to 800 °C in a nitrogen atmosphere. For comparison, pure insulin and pure CaPi were also examined as the controls.

XRD

The obtained BINP solids were examined using an X'Pert PRO (PANalytical, Holland) with monochromatized Cu Kα radiation at a scanning rate of 4°/min over a 2θ range of 10°-60°.

Loading efficiency

The insulin concentrations in DMEM could be measured precisely using a Bicinchoninic Acid (BCA) Protein Assay Kit (Beyotime Institute of Biotechnology, China). Seven insulin solutions with different concentrations of 0, 0.025, 0.05, 0.1, 0.2, 0.4 and 0.5 mg/mL were prepared in DMEM as the standards. Before and after the biomineralization treatment, the free insulin concentrations in the DMEM solutions were measured. The loading efficiency of insulin, P, was estimated using the following formula, where ΔC is the concentration difference and C_0 is the original insulin concentration before the modification: $P = \Delta C/C_0 \times 100\%$.

BINP stability

BINP has UV light absorbance at approximately 320 nm in an aqueous solution, and its concentration in DMEM was tracked *in situ* with a UV-visual spectroscope in real time. During the examination, the pH of the solution was adjusted periodically by 1.0 M HCl, and the relationship between OD_{320} and pH was recorded.

Bioactivity of insulin

The pharmacopoeial method employed to test the potency of insulin includes a single subcutaneous injection of insulin in mice followed by blood glucose determination at 30 min.

Fluorescent labeling of insulin

Synthesis of FITC-labeled insulin was performed based on the reaction between the isothiocyanate group of FITC and the primary amino group of the insulin protein [29]. First, 20 mg of insulin was added to 10 mL of 1.0 M Tris-HCl (pH = 7.4). Then, 3 mg of fluorescein isothiocyanate (FITC, Sigma-Aldrich) dissolved in 3 mL of DMSO was added to the protein solution and stirred slowly at 4 °C overnight. Fluorescent-labeled insulin (FITC-insulin) was purified through dialysis. Prepared FITC-insulin was lyophilized and dissolved in Tris-HCl for subsequent experiments.

In vitro assessments

Cell culture

HepG2 cell lines (human hepatoma cells) were obtained from a standard stock culture (Cell Bank, Chinese Academy of Sciences, Shanghai) and used for *in vitro* study. The HepG2 cells were cultured on tissue culture dishes in DMEM supplemented with 10% fetal bovine serum (FBS, Zhejiang Tianhang Bio-Technique Co., Ltd., China), 50 mg/mL penicillin and 50 mg/mL streptomycin at 37 °C with 5% CO_2.

Insulin resistant cells

R-HepG2 cells were established using a method described by Hideyuki [30]. In our experiments, the HepG2 cells were plated in six-well plates at a density of 1×10^5 cells per well in growth medium. After 24 h, the medium was changed to 10% FBS DMEM with 10^{-6} M dexamethasone (Alfa Aesar, USA) for another incubation period of 60 h to establish R-HepG2.

BINP internalization

R-HepG2 cells were treated in serum-free DMEM overnight, after which the cell culture medium was removed, and the same amount of the biomineralized insulin solution was added. The cells were incubated at 37 °C and 5% CO_2 for 4 h. After the incubation, the solution was removed, and the cells were washed three times using phosphate-buffered saline (PBS, pH = 7.4). The cells were also washed with 0.03% ethylene diamine tetraacetic acid (EDTA) solution to remove any residual complexes.

Flow cytometry analysis

After the treatment with FITC-labeled BINP for 0, 0.5, 1, 2, 3 and 4 h, the cells were collected after being detached with 0.25% trypsin and washed with 5 mM EDTA solution. Then, the cells were washed once with 2 mL of PBS and resuspended with 500 μL PBS at a density of 2×10^6 cells per mL. The cell suspension was analyzed under a flow cytometer equipped with an argon ion laser and filter settings for FITC (530 nm) (Cytomics FC 500 MCL, Beckman Coulter, USA). Data analyses were performed using Flowjo 2.0 software.

MTT assays

HepG2 cells were seeded onto 96-well plates at a density of 2×10^3 cells per well and cultivated in 100 μL of growth medium. After 24 h, the medium was changed to 10% FBS DMEM, with 10-6 M dexamethasone, for 60 h of incubation. Then, the induced medium was removed from each well and replaced with 100 μL of calcium phosphate, insulin and BINP DMEM solution. After 4 h of incubation, the culture medium was replaced with fresh medium. The plates were then returned to the incubator and maintained in 5% CO_2 at 37 °C. Each condition was tested at least eight times. After 24 h of incubation, the culture medium was removed, and 10 μL of 5 mg/mL MTT (3-(4,5-Dimethylthiazol-2-yl)-2,5-diphenyltetrazolium bromide, Sigma-Aldrich, USA) solution was added to 100 μL of fresh medium. The plates were returned to the incubator and maintained in 5% CO_2 at 37 °C for 4 h. The growth medium and excess MTT in each well was removed, and 200 μL of DMSO was then added to each well to dissolve the internalized purple formazan crystals. The plates were assayed at

490 nm using a microplate reader (EON, Bio-tek Instruments, USA). The results were expressed as a percentage of the absorbance of the blank.

Confocal laser scanning microscopy

After the BINP treatment, the cells were fixed with 4% (v/v) formaldehyde at room temperature for 10 min. The fixed cells were then stained by adding 1.5 mL of a solution containing 1 μg/mL 4',6-diamidino-2-phenylindole (DAPI) in the dark to for 5 min. Then, they were washed with PBS, and the cells were observed under a confocal laser scanning microscope (Zeiss LSM-510, Carl Zeiss MicroImaging, Germany). Biomineralized FITC-labeled insulin was identified through this examination.

Negatively stained TEM

After the BINP treatment, the cells were washed with PBS and detached with 0.25% trypsin and 0.05% EDTA for 5 min, pre-fixed with 2.5% glutaraldehyde and 2% paraformaldehyde, post-fixed with 1% osmium tetroxide, dehydrated with a series of alcohols, and infiltrated with resin. The resin sample block was trimmed and thin-sectioned to a thickness of 70 nm for TEM observation.

Glucose detection

Glucose concentrations were detected with a Glucose Oxidase Assay Kit. Glucose oxidase (GOD) converts glucose to gluconic acid and hydrogen peroxide. Hydrogen peroxide formed in this reaction in the presence of peroxidase (POD) oxidatively coupled with 4-aminoantipyrine/phenol to produce red quinonimine dye, which had a maximum absorbance at 505 nm. Biomineralization without insulin or with inactive insulin was performed as control experiments.

RT-PCR

RNA isolation was performed by lysing cells with TRIzol reagent, followed by the addition of chloroform to obtain RNA through centrifugation. cDNA synthesis was performed using the iScript Select cDNA Synthesis Kit. PCR expressions of the IRS-1, IRS-2, Glut-2, and Glut-4 genes were quantified using the MyiQ Single Color RT-PCR machine with SYBR Green detection reagents. The human 18Sr gene served as a housekeeping gene for the normalization of cDNA among samples. The following gene primer sequences were given:

IRS-1, 5′-AGAACTCACTCGGCAGGCACATC-3′ and 5′-TGGTGGGTAGGCAGGCATCATCT-3′;

IRS-2, 5′-CAGCACTGTTTCAGCCCGAAGCT-3′ and 5′-GCAGGTGACCTTGCCTTGTTGGT-3′;

Glut-4, 5′-TCGACCAGCATCTTCGAGACAG-3′ and 5′-CCACCAACAACACCGAGACCAA-3′;

Glut-2, 5′-AGGCAGGGCGACGTTCTCTCTTT-3′ and 5′-TCAGCAGCACAAGTCCCACTGACA-3′;

18Sr, 5′-GACTCAACACGGGAAACCTCAC-3′ and 5′- CCAGACAAATCGCTCCACCAAC-3′.

In vivo animal assessments

Animal

All animal experiments were independently performed by the Laboratory Animal Center of Zhejiang University and the Laboratory Animal Center of Zhejiang Chinese Medical University. The experiments were performed ethically and followed approved protocols. Eight-week-old genetically diabetic KKAy mice (HFK Bioscience, China) were used for the experiments. These mice were fed powdered chow consisting of 48% carbohydrates, 17% protein, 34% fat, 1% fiber, minerals, and vitamins (HFK Biosciencem, China); water was given ad lib. Meanwhile, normal C57BL mice were purchased from the Slaccas Laboratory Animal Centre (China).

BINP Administration

After a two-week pretreatment period, male KKAy mice (age: 10 weeks) weighing 34.0±0.4 g were randomly divided into three groups consisting of 8-12 mice each. The animals in the control group were intraperitoneally injected with 100 μL DMEM, whereas the two treated groups were intraperitoneally injected with 100 μL of DMEM solution containing insulin (40 μg /mL) or *in situ* biomineralization modified insulin (the total insulin concentration was 40 μg/mL, in which 11% was in BINP form). Throughout the experiments, the mice were housed in plastic cages with regulated temperature (24±1 °C) and relative humidity (55±5%) and alternating 12 h light/dark cycles (light: 08:00-20:00). The daily injection (09:00) continued for 2 weeks, and then, the oral glucose tolerance test (OGTT) was used to follow the post-treatment blood glucose levels.

Oral glucose tolerance test (OGTT)

During our experiments, the abilities of the animals to regulate their glucose metabolisms were quantified by OGTT once per week as follows: all mice were orally given a sucrose solution (3 g/kg) using a stomach tube following a 16 h fast, and blood was sampled from the tail vein at 0, 30, 60, 120, and 180 min after the glucose loading. Blood glucose levels were measured with a glucometer (LifeScan OneTouch, USA).

Results

Biomineralization of insulin

The *in situ* biomineralization modification of insulin was simply initiated by adding $CaCl_2$ into the insulin-DMEM solution in which the abundant calcium ions could trigger a spontaneous nucleation of calcium phosphate on acidic amino acid residue on insulin molecules. Biomineralization did not cause any visual changes to the insulin solution (Figure 1A). However, some nanosized particles formed during the modification of the solution. Under transmission electron microscopy (TEM) and scanning electron microscopy (SEM), the resulting particles were found to be spherical and to have an average size of approximately 200 nm (Figure 1B and 1C). Fourier transform infrared spectroscopy (FT-IR) (Figure 1D) indicated the insulin and CaPi components in the particles, and X-ray diffraction (XRD) indicated that the solid phase was in an amorphous state (Figure S1). Thermogravimetric analysis (TGA) revealed that the biomineralized insulin nanoparticles (BINP) contained approximately 5 wt % water, 10 wt % insulin, and 85 wt % CaPi (Figure S2). Synchronous differential scanning calorimetry (DSC) revealed that BINP had heat flow behavior that differed from that of insulin and CaPi (Figure S2). Particularly, the unique endothermic peak of BINP is due to the combined fracture of the insulin and CaPi, implying that BINP was a chemical complex rather than a simple mixture of insulin and CaPi. To validate BINP is a chemical complex, we performed insulin protein labelling using Au nanoparticles. High-resolution transmission electron microscopy (HRTEM) showed that the Au-labelled insulin was encapsulated in the CaPi mineral phase (Figure S3). After the modification, approximately 11% of the original insulin molecules in the solution turned into a form of BINP (Figure S4).

Release of insulin

We explored the release of insulin from BINP. When the particles were exposed to a solution pH<7.2, the release of insulin occurred (Figure 2A). This could be attributed to the dissolution of calcium phosphate particles, leading to dissociation of insulin from BINP (Figure 2B). The calcium phosphate nanophase was stable at pH > 7.2, however, it could be degraded under acidic conditions, particularly at pH < 6.5. Such a pH-dependent behavior is ideal for controllable drug delivery and release in biomedical applications: Generally, the optimized vectors should be stable in extracellular environments (neutral) but dissociated readily by lysosomes (acidic) after cell internalization [31].

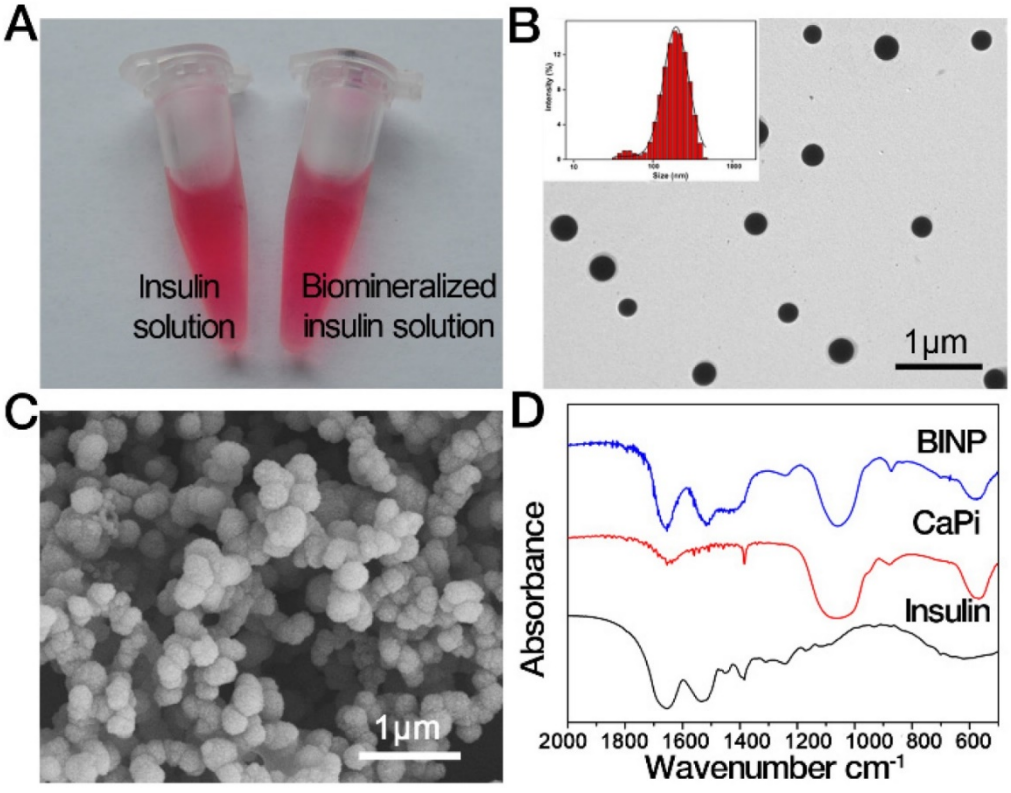

Figure 1. Characterization of biomineralized insulin nanoparticle (BINP). A. Insulin and biomineralized insulin solutions. **B.** TEM (insert: DLS analysis of BINP) and **C.** SEM images of the isolated BINP. **D.** FT-IR of BINP.

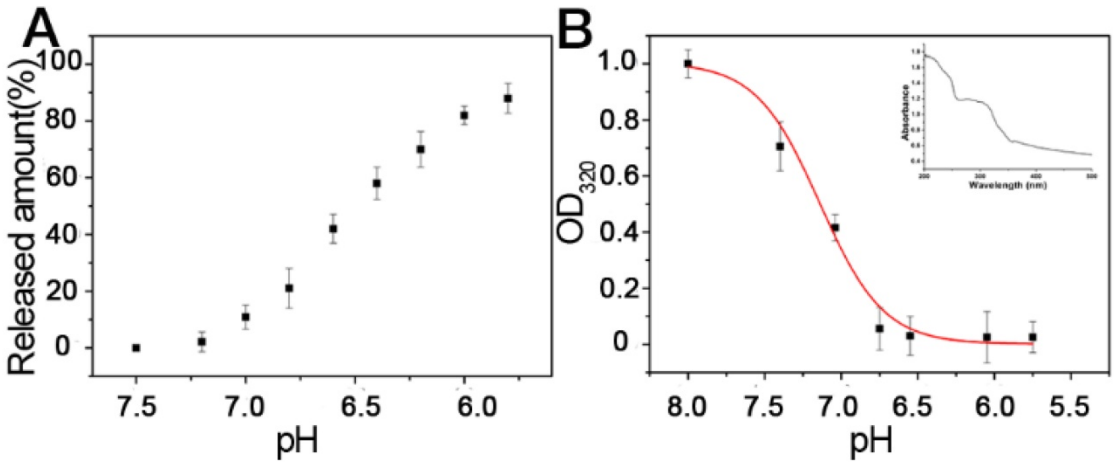

Figure 2. Release of insulin. A. Release profiles of insulin under different pH conditions. **B.** The BINP concentrations were measured using UV absorption at a wavelength of 320 nm. The insert shows a UV spectrum of the BINP solution; the band at approximately 320 nm is attributed to the BINP presence.

Frequently, spontaneous degradation of biological macromolecules in body fluids conditions is a serious roadblock in the widespread application of many protein drugs, including insulin [32]. However, biomineralization engineering could provide an extra protective effect on the enclosed insulin. In a control experiment, the native insulin was damaged by a protease (α-chymotrypsin) within 30 min. In contrast, the insulin in BINP remained contact, without any significant degradation under the exact same experimental conditions (Figure S5). We found that BINP conferred excellent thermostability to enclosed insulin, which could be stored for >1 month in DMEM at 37 °C. Furthermore, the bioactivity of the enclosed insulin remained after the storage (Figure S6). This is because the rigidity of the inorganic matrix can decrease the probability of immobilized proteins to undergo denaturing unfolding-refolding motions [33, 34].

Intracellular delivery

Ineffective uptake is another primary obstacle in using protein drugs. Fortunately, the problem of insulin uptake can be readily overcome by BINP. Although only a small proportion of insulin was biomineralized in the solution, the *in situ* modified solutions (total insulin concentration was 40 μg/mL, in which 11% insulin was biomineralized into BINP) exhibited a distinct characteristic from the originals (40 μg/mL, all were free insulin) in the cell uptake experiments. The liver is an organ targeted by insulin [35]; therefore, we used the liver cell line in our *in vitro* assessments. In this study, insulin was labeled by fluorescein isothiocyanate (FITC). As shown in Figure 3A, there was no detectable intracellular FITC signal in the insulin group, indicating that free insulin in its molecular form was not able to enter cells. Nevertheless, intensive green fluorescence was observed intracellularly when the biomineralized insulin solution was applied (Figure 3B). This followed a large-scale intracellular accumulation of insulin, which contributed to the BINP in the modified solution. The uptake kinetics of BINP were examined quantitatively using flow cytometry (Figure S7). Within only 30 min, 96% of the cells contained insulin. This value reached 100% after 2 h, and the experiment showed that the cellular uptake of BINP was rapid and highly efficient.

To determine a possible entrance pathway of BINP into cells, the cell nuclei and lysosomes were stained using DAPI and LysoTracker Red, respectively. The overlap of green and blue clearly indicated the presence of insulin in the cells (Figure 3C). The overlap of green and red emissions implied that the BINP were transported to lysosomes, from which biomineralized insulin could escape into the cytoplasm. The presence of BINP in the lysosomes indicated an endocytosis pathway for nanoparticle internalization, and the separate detection of intracellular green florescence confirmed the release of nanoparticles from lysosomes into the cytosol. In contrast, the entrance of free insulin molecules into intact cells could not be detected (Figure S8). We noted that the BINP had favorable dimensions (100-200 nm) for endocytosis, in accordance with a well-established understanding of nano biotechnology [36]. The pH-sensitive characteristics of BINP were also in accordance with the observed internalization and subsequent dissociation processes under intracellular conditions. Generally, internalized insulin molecules are typically immediately degraded by insulin-degrading enzyme (IDE) in the cytoplasm [13]. However, the large-scale presence of insulin signals within the cells demonstrated the stability of biomineralized insulin under intracellular conditions,

which was due to the protective effect of BINP on the insulin molecules. The application of BINP affords the possibility of exploring the intracellular functions of insulin molecules; therefore, we examined the assumption that the administration of intracellular insulin might lead to a different therapeutic effect than that of membrane-bound insulin.

In vitro assessment

Insulin resistance is defined as a change in physiological regulation such that a fixed dose of insulin does not affect glucose metabolism to the extent that it does in normal individuals [37]. R-HepG2 was obtained using an established method [30], and its glucose metabolism was measured to be approximately 50% of normal HepG2; normal HepG2 was used as a control, and its glucose metabolism was defined as 100%.

After the treatment of insulin or BINP for 4 h, the medium was changed to DMEM (low glucose, without phenol), and the glucose concentration was measured periodically using a Glucose Oxidase Assay Kit. Using free insulin treatment, the cellular glucose metabolism of R-HepG2 increased transiently to 70% (t = 0 h) but then dropped quickly. At t = 48 h, the free insulin treated cells returned to their original insulin-resistant state. This phenomenon was consistent with the short-term effect of insulin on diabetes. Using BI treatment, the instantaneous glucose metabolism increased to approximately 70%, and surprisingly, this upregulation effect is long term (Figure 4A). Post-treatment, the glucose metabolism still increased, reaching 112% at t = 72 h. R-HepG2 cells reversed to normal HepG2 through BINP, based upon the disappearance of insulin resistance symptoms. Furthermore, this enhancement could be inherited in the daughter cells of R-HepG2 cells after a few generations (Figure 4B). Note that in our parallel control experiments, calcium phosphate nanoparticles without insulin or with inactive insulin were inert in terms of any glucose metabolism regulations (Figure S9). Thus, the observed long-term improvement should be attributed to the intracellular insulin delivered through biomineralization.

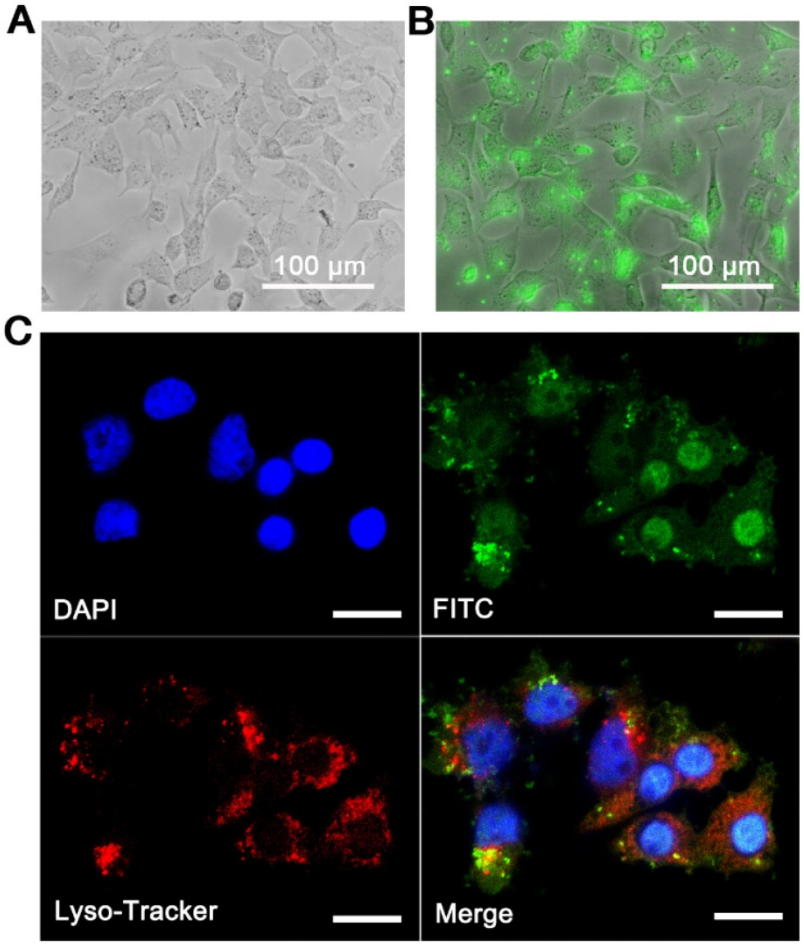

Figure 3. Intracellular localization of insulin through the delivery of BINP. Fluorescence microscopy images of R-HepG2 after **A.** Insulin treatment and **B.** Biomineralization treatment with FITC-labeled insulin molecules (FITC-BINP). **C.** Confocal laser scanning microscopy images of R-HepG2 after the FITC-BINP treatment (green), DAPI-stained nuclei (blue) and LysoTracker (red) (bar = 20 μm).

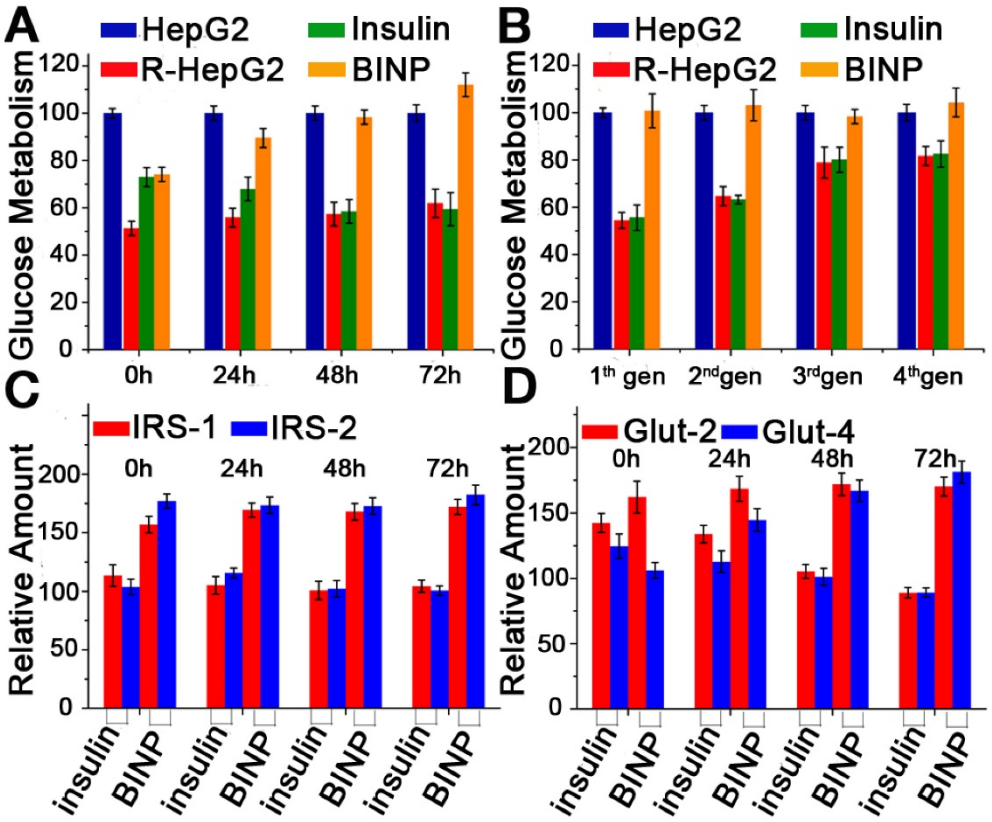

Figure 4. *In vitro* assessments of BINP. A. Glucose metabolism abilities of untreated HepG2 (HepG2), untreated R-HepG2 (R-HepG2), insulin-treated R-HepG2 (Insulin) and BINP-treated R-HepG2 (BINP) post-treatment. The values of HepG2 cells in the control experiments are defined as 100%. Data are shown as the mean ± s.d. of biological replicates (n = 10). **B.** Glucose metabolisms of the untreated and treated cells after passaging. The values of the HepG2 cells in the control experiments are defined as 100% (n = 10). Relative mRNA amounts of **C.** IRS-1 and IRS-2 **D.** Glut-2 and Glut-4 in R-HepG2 cells after the insulin and BINP treatments; the corresponding values of untreated R-HepG2 cells were defined as 100%. The statistical significance of differences among different groups was analyzed using Student's t -test as implemented in SPSS (Statistical Product and Service Solutions) software. The difference between insulin group and BINP group after t = 0 h is significant (*** $p < 0.001$).

The evaluation of mRNA expression through real-time polymerase chain reaction (RT-PCR) further validated the potential of BINP as long-term molecular glucose controls. Traditionally, the action of insulin is mediated through the insulin receptor (IR) [9, 38]. The level of tyrosine kinase activity reflects the serum concentration of insulin, and tyrosine kinase activity appears to mediate the insulin response through tyrosine phosphorylation of the receptor itself and the insulin receptor substrate (IRS) [39]. IRS proteins are the adapter molecules in the insulin signaling process, and they couple with the insulin receptor upstream, while PI3K-PKB and MAPK act as downstream kinases [40]. PI3K regulates the activity of the glucose transporter (Glut), which is a rate-limiting step of glucose transport, use, and storage [41]. When cells become insulin resistant, the downregulation in IRS mRNA causes insulin signaling dysfunction, and the level of Glut mRNA decreases accordingly. There are several isoforms of IRS and Glut, of which IRS-1 mRNA, IRS-2 mRNA, Glut-2 mRNA, and Glut-4 mRNA were examined through RT-PCR in our experiments due to their relative abundance. For each experiment, the corresponding mRNA in the untreated R-HepG2 cells was used as a standard. Insulin induced an immediate increase in the levels of all four mRNAs compared with the controls, but the expression levels of the four mRNAs dropped after treatment (Figure 4C and 4D). At t = 72 h, the mRNA expression levels of the insulin treatment group were even lower than those of the untreated group. In contrast, the mRNA expression levels induced by BINP remained at their increased levels throughout the experiment, representing the long-term upregulation of glucose metabolism after treatment (Figure 4C and 4D). Thus, the upregulated expression levels induced by biomineralized insulin became permanent, whereas those induced by free insulin were temporary; the results aligned with those of the glucose metabolism experiments.

In vivo assessment

The therapeutic effect of BINP on diabetes was also confirmed *in vivo* through animal experiments. KKAy mice are widely used as type 2 diabetes models. These mice are established by the

introduction of the yellow obese gene into mice of the diabetic KK strain, and they exhibit obesity-related hyperglycemia, hyperlipidemia, and hyperinsulinemia [42]. The diabetes symptoms of KKAy mice were confirmed prior to our experiments, and the mice were randomly divided into three groups with 8-12 mice each: 1) no treatment (KKAy), 2) insulin treatment (Insulin), and 3) BINP treatment (BINP). The control group contained normal, healthy C57BL mice (C57). Mice in the treatment groups received daily intraperitoneal injections of 100 μL of DMEM solution containing insulin or BINP for a continuous treatment period of two weeks. After treatment withdrawal, the ability of the animals to regulate their glucose metabolisms was quantified by an oral glucose tolerance test (OGTT) that was administered periodically. The insulin treatment group exhibited no difference from the KKAy group because the temporary therapeutic effect of insulin vanished quickly and completely after the end of the treatment. This phenomenon aligned with the traditional understanding of the effect of insulin on diabetes. However, the BINP treatment group exhibited long-term improvements in their glucose metabolisms: within three weeks after the treatment, the blood glucose levels of the mice in the BINP group were controlled as adequately as those of the healthy C57 mice (Figure 5A-D). This result could imply a recovery from diabetes after biomineralized insulin therapy. Two different animal laboratories confirmed the provided OGTT results independently (Figure S10), and both reported the advantages of treatment with BINP over traditional insulin for diabetes.

In vivo tissue localization of BINP showed that liver was the major target organ during the treatment (Figure S11), which was coincident with the distribution feature of pure nano-CaPi vectors [43]. Usually, the intraperitoneal injected drug can be absorbed through the mesenteric vein in the abdomen and then gradually passes into the systemic circulation [44, 45]. The observation also indicated that the injected BINP particles could be completely depredated within 24 h after the administration. Together with the *in vitro* results, the study followed that the long-term treatment of the diabetes mice should be attributed to the BINP-induced intracellular targeted treatment rather than the release of free insulin from BINP. Moreover, it should be emphasized that in our animal assessments, the modified insulin solution was used directly. During the experiments, no significant side effect was detected in the group of BINP-treated mice. However, as with any other new technology or material, the manufacturing process and safety profile should be carefully evaluated before using biomineralized insulin in clinical developments.

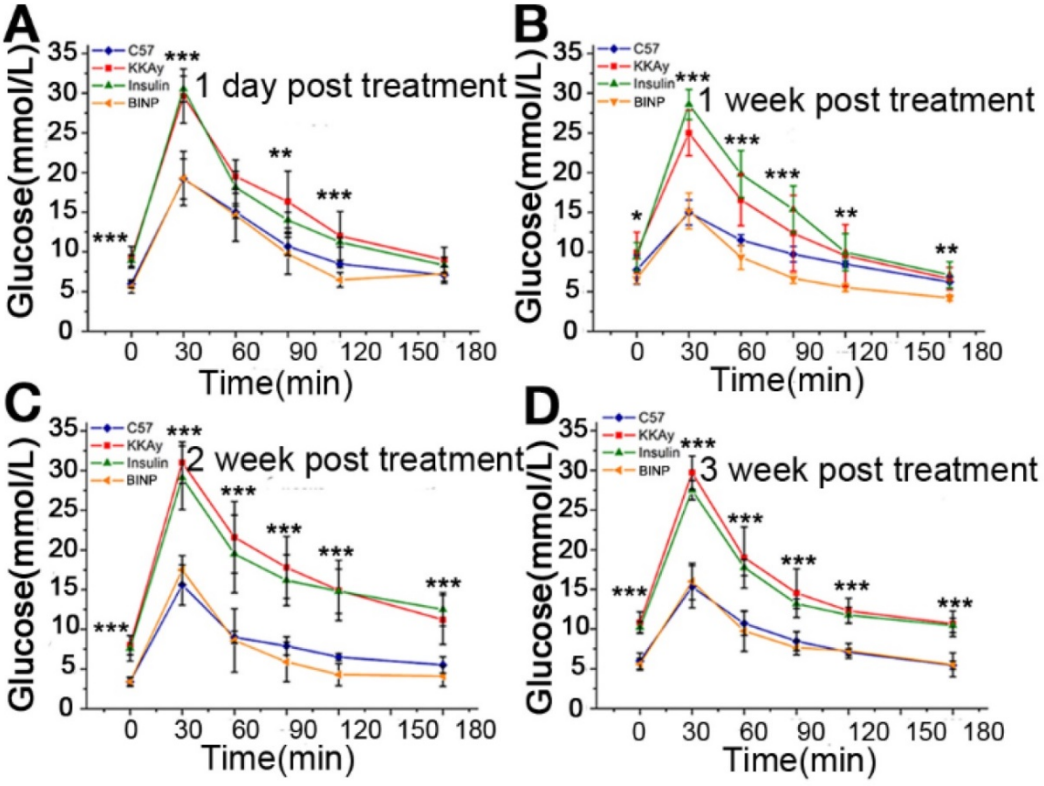

Figure 5. *In vivo* assessments of BINP. A. - D. OGTT results of the healthy (C57), diabetic (KKAy), insulin-treated diabetic (insulin), and biomineralized insulin-treated diabetic (BINP) mice post-treatment. The statistical significance of differences among different groups was analyzed using Student's t -test as implemented in SPSS (Statistical Product and Service Solutions) software (* $p < 0.05$, ** $p < 0.01$, *** $p < 0.001$, ns, not significant).

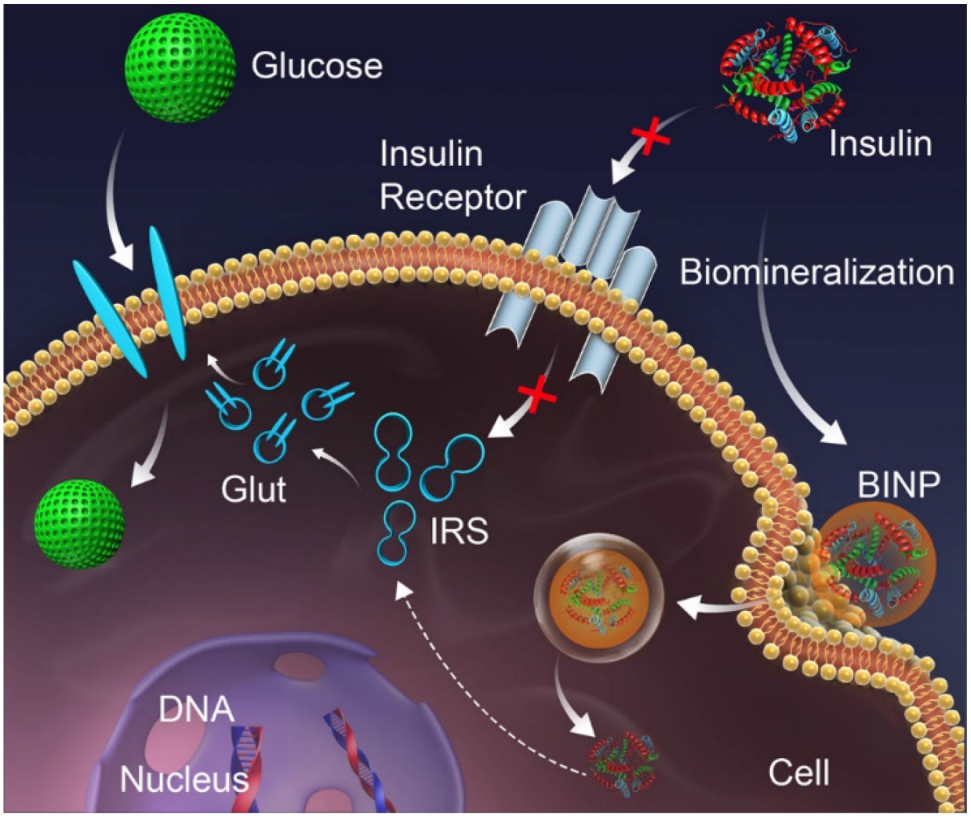

Figure 6. Schematic of the long-term effect of BINP. The conventional action of insulin on the cell membrane (red pathway) is inhibited by an insufficient number of receptors, resulting in type 2 diabetes; the *in situ* biomineralization of insulin (green pathway) delivers insulin into the intact cell through BINPs, triggering an intercellular action that stimulates glucose metabolism.

Discussion

The biological effects of insulin are conventionally generated as a direct result of insulin binding to specific receptors on the plasma membranes of cells [7]. External insulin, commonly injected subcutaneously, has a short-term effect on diabetes treatment [46], which was confirmed by our control experiments. It is generally accepted that the internalization of insulin by intact cells is inefficient [13]. However, the *in situ* biomineralization of insulin can result in nanoparticles of insulin-CaPi complex that can bypass the cell membrane *via* endocytosis. Meanwhile, the biosecurity of calcium phosphate nanoparticle was confirmed. It has already been demonstrated experimentally that the influence of calcium phosphate nanoparticle on cell viability is limited at low concentration of Ca^{2+} in our previous study [47]. Moreover, the MTT assays in our study indicated that the BINP did not affect cell viability (Figure S12), which suggests that biomineralization is an important method for protein delivery with potential applications in the clinic.

The biomineralization-assisted insulin treatment of diabetes encompasses four stages: 1) insulin condensation and complexation with a mineralized CaPi phase to generate BINP, 2) internalization of BINP by endocytosis, 3) escape of BINP from lysosomes into the cytosol, and 4) insulin action in the cells (Figure 6). The endocytosis and intercellular delivery of BINP can also be demonstrated by a TEM image (Figure S13) showing the presence of the nanoparticles within the cells. However, the detailed mechanism involved with the intracellular treatment effect of insulin still needs further in-depth exploration. Nevertheless, the experimental results have demonstrated that the biomineralization modification can transport insulin molecules into the cells at large scales to stimulate a long-term effect for diabetes treatment within cells, in contrast with the temporary effect of insulin that binds to cell membranes.

This interesting phenomenon may be an alternative strategy for type 2 diabetes treatment. This study also provides a successful demonstration of the advantages of nanomaterials in biomedical practice. The efficient internalization and protection of insulin are achieved by its modified form, even though the isolated insulin molecule is unstable under intracellular conditions and is unable to provide internal stimulation. We highlight that biomineralization is a particularly useful tool. The *in*

situ biomineralization of insulin is feasible, biocompatible, and cost effective. We believe that the example of diabetes treatment through biomineralized insulin can be applied to the treatments of other diseases, and we encourage the use of biomineralization as a general medicine improvement strategy.

Abbreviations

CaPi: calcium phosphate; BINP: biomineralized insulin nanoparticles; DMEM: Dulbecco's Modified Eagle Medium; PBS: phosphate buffer saline; TEM: transmission electron microscopy SEM: scanning electron microscopy; DLS: dynamic light scattering; FT-IR: Fourier transform infrared; TGA/DSC: thermogravimetric analysis/differential scanning calorimetry; XRD: X-ray diffraction; BCA: bicinchoninic acid; FITC: fluorescein isothiocyanate; DMSO: dimethyl sulfoxide; FBS: fetal bovine serum; R-HepG2: insulin resistant HepG2; DAPI: 4',6-diamidino-2-phenylindole EDTA: tetraacetic acid; MTT: 3-(4,5-Dimethylthiazol-2-yl)-2,5-diphenyltetrazolium bromide; GOD: glucose oxidase; POD: peroxidase; RT-PCR: reverse transcription PCR; cDNA: complementary DNA; mRNA: messenger RNA; IRS: insulin receptor substrate; IR: insulin receptor Glut: glucose transporter; OGTT: oral glucose tolerance test; IDE: insulin-degrading enzyme.

Supplementary Material

Supplementary figures.
http://www.thno.org/v07p4301s1.pdf

Acknowledgements

We thank YH. C and W. C for their help with the experiments and analyses. This work was supported by the Fundamental Research Funds for the Central Universities of China, the National Natural Science Foundation of China (91127003) and Zhejiang Provincial Natural Science Foundation of China (Y17B010009).

Authors' Contributions

RK.T initiated the study of biomineralized insulin. Y.X and RK.T designed the experiments. Y.X, XY.W and XY.L performed the experiments. Y.X., B.W, XR.X and RK.T interpreted the data. Y.X and RK.T wrote the manuscript.

Competing Interests

The authors have declared that no competing interest exists.

References

1. Zimmet P, Alberti K, Shaw J. Global and societal implications of the diabetes epidemic. Nature. 2001; 414: 782-7.
2. Kahn SE, Hull RL, Utzschneider KM. Mechanisms linking obesity to insulin resistance and type 2 diabetes. Nature. 2006; 444: 840-6.
3. Samuel VT, Shulman GI. Mechanisms for insulin resistance: common threads and missing links. Cell. 2012; 148: 852-71.
4. Gómez-Pérez FJ, Rull JA. Insulin therapy: current alternatives. Archives of Medical research. 2005; 36: 258-72.
5. Nathan DM, Buse JB, Davidson MB, Ferrannini E, Holman RR, Sherwin R, et al. Medical management of hyperglycemia in type 2 diabetes: a consensus algorithm for the initiation and adjustment of therapy. Clinical Diabetes. 2009; 27: 4-16.
6. Gu Z, Aimetti AA, Wang Q, Dang TT, Zhang Y, Veiseh O, et al. Injectable nano-network for glucose-mediated insulin delivery. ACS nano. 2013; 7: 4194-201.
7. Saltiel AR, Kahn CR. Insulin signalling and the regulation of glucose and lipid metabolism. Nature. 2001; 414: 799-806.
8. Yu J, Zhang Y, Ye Y, DiSanto R, Sun W, Ranson D, et al. Microneedle-array patches loaded with hypoxia-sensitive vesicles provide fast glucose-responsive insulin delivery. Proceedings of the National Academy of Sciences. 2015; 112: 8260-5.
9. White M, Kahn C. The insulin signaling system. J biol Chem. 1994; 269.
10. O'Brien RM, Granner DK. Regulation of gene expression by insulin. Physiological Reviews. 1996; 76: 1109-61.
11. Duckworth WC, Bennett RG, Hamel FG. The significance of intracellular insulin to insulin action. Journal of investigative medicine: the official publication of the American Federation for Clinical Research. 1997; 45: 20-7.
12. Miller DS. Stimulation of RNA and protein-synthesis by intracellular insulin. Science. 1988; 240: 506-9.
13. Duckworth WC, Bennett RG, Hamel FG. Insulin degradation: progress and potential 1. Endocrine reviews. 1998; 19: 608-24.
14. Brandimarti P, Costa-Júnior JM, Ferreira SM, Protzek A, Santos G, Carneiro EM, et al. Cafeteria diet inhibits insulin clearance by reduced insulin-degrading enzyme expression and mRNA splicing. Journal of Endocrinology. 2013; 219: 173-82.
15. Valera Mora ME, Scarfone A, Calvani M, Greco AV, Mingrone G. Insulin clearance in obesity. Journal of the American College of Nutrition. 2003; 22: 487-93.
16. Birch JR, Onakunle Y. Biopharmaceutical proteins: opportunities and challenges. Therapeutic proteins: Methods and protocols. 2005: 1-16.
17. Bamrungsap S, Zhao Z, Chen T, Wang L, Li C, Fu T, et al. Nanotechnology in therapeutics: a focus on nanoparticles as a drug delivery system. Nanomedicine. 2012; 7: 1253-71.
18. Gu Z, Biswas A, Zhao M, Tang Y. Tailoring nanocarriers for intracellular protein delivery. Chemical Society Reviews. 2011; 40: 3638-55.
19. Torchilin VP. Recent advances with liposomes as pharmaceutical carriers. Nature reviews Drug discovery. 2005; 4: 145-60.
20. Panyam J, Zhou W-Z, Prabha S, Sahoo SK, Labhasetwar V. Rapid endo-lysosomal escape of poly (DL-lactide-co-glycolide) nanoparticles: implications for drug and gene delivery. The FASEB Journal. 2002; 16: 1217-26.
21. Kam NWS, Dai H. Carbon nanotubes as intracellular protein transporters: generality and biological functionality. Journal of the American Chemical Society. 2005; 127: 6021-6.
22. Chen J, McLellan JM, Siekkinen A, Xiong Y, Li Z-Y, Xia Y. Facile synthesis of gold− silver nanocages with controllable pores on the surface. Journal of the American Chemical Society. 2006; 128: 14776-7.
23. Mann S. Biomineralization: principles and concepts in bioinorganic materials chemistry. Oxford University Press. 2001.
24. Wilt FH. Developmental biology meets materials science: morphogenesis of biomineralized structures. Developmental biology. 2005; 280: 15-25.
25. Meyers MA, Chen P-Y, Lopez MI, Seki Y, Lin AY. Biological materials: A materials science approach. Journal of the mechanical behavior of biomedical materials. 2011; 4: 626-57.
26. Palmer LC, Newcomb CJ, Kaltz SR, Spoerke ED, Stupp SI. Biomimetic systems for hydroxyapatite mineralization inspired by bone and enamel. Chemical reviews. 2008; 108: 4754-83.
27. Dorozhkin SV, Epple M. Biological and medical significance of calcium phosphates. Angewandte Chemie International Edition. 2002; 41: 3130-46.
28. Xie J, Zheng Y, Ying JY. Protein-directed synthesis of highly fluorescent gold nanoclusters. Journal of the American Chemical Society. 2009; 131: 888-9.
29. Caruso F, Möhwald H. Protein multilayer formation on colloids through a stepwise self-assembly technique. Journal of the American Chemical Society. 1999; 121: 6039-46.
30. Sakoda H, Ogihara T, Anai M, Funaki M, Inukai K, Katagiri H, et al. Dexamethasone-induced insulin resistance in 3T3-L1 adipocytes is due to inhibition of glucose transport rather than insulin signal transduction. Diabetes. 2000; 49: 1700-8.
31. Iversen T-G, Skotland T, Sandvig K. Endocytosis and intracellular transport of nanoparticles: present knowledge and need for future studies. Nano Today. 2011; 6: 176-85.
32. Frokjaer S, Otzen DE. Protein drug stability: a formulation challenge. Nature reviews drug discovery. 2005; 4: 298-306.

33. Cao A, Ye Z, Cai Z, Dong E, Yang X, Liu G, et al. A facile method to encapsulate proteins in silica nanoparticles: encapsulated green fluorescent protein as a robust fluorescence probe. Angewandte Chemie International Edition. 2010; 49: 3022-5.
34. Ravindra R, Zhao S, Gies H, Winter R. Protein encapsulation in mesoporous silicate: the effects of confinement on protein stability, hydration, and volumetric properties. Journal of the American Chemical Society. 2004; 126: 12224-5.
35. Puigserver P, Rhee J, Donovan J, Walkey CJ, Yoon JC, Oriente F, et al. Insulin-regulated hepatic gluconeogenesis through FOXO1–PGC-1α interaction. Nature. 2003; 423: 550-5.
36. Sahay G, Alakhova DY, Kabanov AV. Endocytosis of nanomedicines. Journal of controlled release. 2010; 145: 182-95.
37. Alberti KGMM, Zimmet Pf. Definition, diagnosis and classification of diabetes mellitus and its complications. Part 1: diagnosis and classification of diabetes mellitus. Provisional report of a WHO consultation. Diabetic medicine. 1998; 15: 539-53.
38. Schlessinger J. Cell signaling by receptor tyrosine kinases. Cell. 2000; 103: 211-25.
39. Taniguchi CM, Emanuelli B, Kahn CR. Critical nodes in signalling pathways: insights into insulin action. Nature reviews Molecular cell biology. 2006; 7: 85-96.
40. Sun XJ, Wang L, Zhang Y. Role of IR5-2 in insulin and. Nature. 1995; 377: 173.
41. Mueckler M. Facilitative glucose transporters. European Journal of Biochemistry. 1994; 219: 713-25.
42. Suto J-i, Matsuura S, Imamura K, Yamanaka H, Sekikawa K. Genetic analysis of non-insulin-dependent diabetes mellitus in KK and KK-Ay mice. European Journal of Endocrinology. 1998; 139: 654-61.
43. Roy I, Mitra S, Maitra A, Mozumdar S. Calcium phosphate nanoparticles as novel non-viral vectors for targeted gene delivery. International Journal of Pharmaceutics. 2003; 250: 25-33.
44. Porrino LJ. Functional consequences of acute cocaine treatment depend on route of administration. Psychopharmacology. 1993; 112: 343-51.
45. Myers CE, Collins JM. Pharmacology of intraperitoneal chemotherapy. Cancer investigation. 1983; 1: 395-407.
46. Burge MR, Schade DS. Insulins. Endocrinology and metabolism clinics of North America. 1997; 26: 575-98.
47. Liu Z, Xiao Y, Chen W, Wang Y, Wang B, Wang G, et al. Calcium phosphate nanoparticles primarily induce cell necrosis through lysosomal rupture: the origination of material cytotoxicity. Journal of Materials Chemistry B. 2014; 2: 3480-9.